12-2011

# Opacity of P(MMA-MAA)-PMMA Composite Latex System with Varying MAA Concentration

Gilbert U. Yu

Jerry T. Dy

Erwin P. Enriquez

**Philippine Journal of Science**
140 (2): 221-230, December 2011
ISSN 0031 - 7683
Date Received: 19 Feb 2009

# Opacity of P(MMA-MAA)-PMMA Composite Latex System with Varying MAA Concentration

**Gilbert U. Yu***, **Jerry T. Dy**, and **Erwin P. Enriquez**

Department of Chemistry, School of Science and Engineering,
Ateneo de Manila University, Loyola Heights, Quezon City, Philippines 1108

**Polymer composites of core-shell morphology are commonly used in the paint industry as opacity enhancer. These are usually made of block copolymer systems wherein the core is formed from a polymer that swells in the presence of a solvent and surrounded by a high glass transition polymeric shell. Thus, upon drying, the swollen regions turn into voids while leaving a hard shell. Here, composites based on poly(methyl methacrylate-butyl acrylate) [P(MMA-BuA)] (seed stage), poly(methyl methacrylate-methacrylic acid) [P(MMA-MAA)] (second stage), and poly(methyl methacrylate) [PMMA] (third stage) were synthesized through a multistage sequential emulsion polymerization and their opacity was investigated. The second stage formulation of P(MMA-MAA) system was varied by changing the methyl methacrylate (MMA): methacrylic acid (MAA) mole composition, and the dried films of these composite latexes were characterized by infrared spectroscopy (IR), differential scanning calorimetry (DSC), and atomic force microscopy (AFM). The AFM images and ammonium hydroxide ($NH_4OH$) swelling studies confirmed the successful incorporation of the seed (first) stage with the second and third stage polymerization with PMMA. The differences in PMAA concentrations among the second stage polymer compositions were determined from the IR spectra and glass transition temperature ($T_g$) data. Investigations on the opacity and hiding power of these polymer composites were done using optical densitometry. The results show increasing absorbance, indicating increasing opacity, with increasing polymethacrylic acid (PMAA) concentration in the second stage composition.**

Key Words: core-shell, emulsion polymerization, latex morphology, opacity

## INTRODUCTION

Multistage emulsion polymerization is a well-established technique used in preparing multiphase polymer composites with well-defined morphologies (Dimonie et al. 1997; El-Asser et al. 1997; Winnik 1997). Of the several polymer particles that one can formulate out of this process, core-shell polymers are highly investigated. These materials possess an architecture appealing for use in several industrial applications. Unlike blends of two or more polymers that have properties somewhere in between the characteristics of the polymers incorporated, core-shell polymer latexes can have "core" polymers that behave differently from its "shell (Vanderhoff et al. 1992)." Several factors affect the structure of the multistage sequential polymerization particles produced: the type and amount of surfactants used, type of initiator added, mode of monomer addition, and degree of cross-linking among others (Dimonie et al. 1997; Okubo et al. 1992). Because of this, synthesis of core-shell latexes does not always result in ideal core-shell morphology with complete phase separation (Dimonie et al. 1997; Vanderhoff et al. 1992; Park 2000; Sunberg et al. 2008; Cao et al. 2005).

*Corresponding author: g78red@yahoo.com

The unique structure and superior performance of these multistage polymer particles give rise to a variety of uses (Kasper et al. 1998; Landfester et al. 1996; Dimonie et al. 1997). Such latexes are already being used in the paint, ink, paper, and plastic industry (MacDonald et al. 2002) as performance additives that function as impact resistant modifiers and toughening agents (Zhong et al. 1998; Kirsch et al. 1999) as well as opacifiers and gloss enhancers (Straus, 1987). Poly(methyl methacrylate-methacrylic acid-butyl acrylate) [P(MMA-MAA-BuA)] core-shell latexes, for example, have properties that enhance the opacity of the paint, ink, or coated paper (Cao et al. 2005). It has been demonstrated that the formulation and the architecture of these particles affect their hiding power, and efforts were focused on establishing processes to improve the stability of these particles (Vanderhoff et al. 1992). Kowalski and co-workers synthesized a P(MMA-MAA- BuA)–PMMA core-shell polymer, wherein the addition of $NH_4OH$, particularly, after multistage polymerization of the monomers, swells the polymethacrylic acid-laden core leaving behind a void upon drying. These voids could provide sufficient contrast in refractive index creating a more opaque polymer film when dried; this implies that core-shell structure is critical for the increased opacity of these latexes (Kowalski et al. 1984).

To our knowledge, only studies on the relationship between shell composition and opacity have been made (Dolui et al. 2008) and no study on the correlation between opacity and MAA composition has been undertaken. In this study, the same P(MMA-MAA- BuA)–PMMA system is used to investigate the effect of varying the MAA composition on the opacity of the dried latexes. In particular, three different latex formulations of variable MMA: MAA monomer ratios were polymerized subsequently with pure PMMA. The structure and composition of these multiphase composite latexes were characterized using Fourier transform infrared (FTIR) spectroscopy, differential scanning calorimetry (DSC), and atomic force microscopy (AFM). The opacity or hiding power of the films or coatings produced was investigated by optical densitometry.

## MATERIALS AND METHODS

Materials used in this study such as methyl methacrylate (MMA), butyl acrylate (BuA), ethylene glycol dimethacrylate (EGDMA), ammonium persulfate (APS), and the surfactants sodium dodecyl benzene sulfonate (SDBS) and nonylphenol ethoxide (NPE) were all of industrial grade. Methacrylic acid (MAA, 98%) and NH4OH (10-35% NH3) were of reagent grade and purchased from Merck-Schuchardt and Univar, respectively. All materials were used as received.

### Synthesis

#### Preparation of the Seed Latex (Stage 1)

A mixture of 120 g of deionized water and 0.70 g of SDBS was stirred continuously in a reaction flask at a rate of 240-260 $min^{-1}$ and heated to 80 °C. A second mixture of monomer emulsion was prepared separately by mixing 11.0 g of distilled, deionized $H_2O$ (17.3 $M\Omega\ cm^{-1}$), 0.12 g of SDBS, 17.26 g of BuA, 15.48 g of MMA, and 0.45 g of MAA in a beaker for 30 min. The second mixture was infused at a flow rate of 700 µL/min simultaneous with 2.5 mL aqueous solution of APS initiator (approximately 6%) delivered separately into the reaction vessel. The reaction was allowed to run for one hour allowing the temperature to reach 85 ±1 °C. The system was allowed to cool and filtered. The pH of the system was increased to 9.5 by addition of $NH_4OH$ solution to the latex.

#### Preparation of the Composite Latex (Stage 2)

Three different sets (Table 1) of 2nd stage polymer latexes were formulated with varying amounts of MAA: 8.92 g, 11.90 g, and 14.87 g (these will be referred to as 73/27, 66/34, and 62/38 mole % MMA: MAA 2nd stage latexes respectively). The reaction vessel was initially charged with 118 g deionized water and 3.52 g of the seed latex from stage 1 with temperature kept at 85 ±1 °C for the entire run. The stirring rate was maintained within the range of 240-300 $min^{-1}$. A 3.50 mL of APS aqueous solution (approximately 7.5%) was placed inside the reactor and concurrently, an emulsion composed of 13.33 g of deionized water, 0.08 g of SDBS, 0.08 g of NPE (nonyl phenol ethoxide), with $NPE_5$, 0.06 g, $NPE_{45}$, 0.02 g, respectively, 27.80 g of MMA, required amounts of MAA, and 0.10 g of the cross-linker, EGDMA, were infused into the reaction vessel via syringe pump at a flow rate of 250-270 µL/min. The polymerization took about 3 hours. After subsequent cooling and filtering, the pH of the polymer emulsion was measured to be 2.0.

#### Preparation of the Composite Latex (Stage 3)

A mixture of 75.0 grams of deionized water and 4.50 grams of the 2nd stage emulsion were placed inside a flask with temperature and stirring rate kept at 85 ±1 °C and 240-300 $min^{-1}$ , respectively. The reaction vessel was charged with 5.00 mL APS aqueous solution (about 1.5%) with MMA infused via two ways. One run had an 18.0-g pure MMA monomer delivered at a flow rate of 300 µL/min which took about one hour. In another run an 18.0-g MMA emulsion with 0.06 g of SDBS was delivered at the same rate. The latexes were allowed to cool and filtered.

**Swelling with NH4OH at High Temperature**

The final stage samples were titrated with concentrated ammonium hydroxide solution to a pH value of about 10, and were allowed to swell overnight. These samples were then heated to 90 °C for one hour to ensure substantial diffusion of the base ($NH_4OH$) to the 2nd stage latex (Okubo et al. 1992).

**Infrared Spectroscopy**

Infrared (IR) analysis was made using a Fourier transform infrared spectrophotometer (Shimadzu FTIR-8210PC). Each of the oven-dried samples of stage 2 and stage 3 particles was pelletized with KBr and analyzed in transmission mode averaging 32 scans at 4 $cm^{-1}$ resolution using a deuterated triglycine sulfate (DTGS) detector.

**Differential Scanning Calorimetry**

Glass transition temperatures ($T_g$) of the dried latex particles were determined using a differential scanning calorimeter (Shimadzu DSC-50). Approximately 5 mg of sample was crimped in an aluminum cell and analyzed under $N_2$ atmosphere at a flow rate of 20 mL/min. All DSC runs for each sample were repeated and $T_g$ values were recorded during the 2nd scan.

**Atomic Force Microscopy**

Atomic force microscopy was done on latex samples using a Topometrix Explorer TMX 2000 with a silicon nitride ($Si_3N_4$) tip of a nominal force constant of 0.2 N/m. Imaging was done in contact mode. About 100 µL of each sample was placed on a cover slip, mounted on a spin coater, and spun at 2085 $min^{-1}$ for 1 minute. These were placed in a petri dish, and were oven dried for 3 hours at 45 °C. The samples were scanned in the AFM, imaging 100 x 100 $\mu m^2$, 25 x 25 $\mu m^2$, and 5 x 5 $\mu m^2$ areas. At least two sites were imaged for each sample. The composite latex particles' size and polydispersity were estimated from the 25 x 25 $\mu m^2$ AFM images for a total of about 900 particles, randomly selected and using the AFM imaging software. The polydispersity or uniformity index is calculated using equation 1:

$$UI = \frac{D_w}{D_n} = \frac{\frac{\sum N_i D_i^4}{\sum N_i D_i^3}}{\frac{\sum N_i D_i}{\sum N_i}} \qquad (1)$$

where $D_w$ is the weight-average diameter, $D_n$ is the number-average diameter, $N_i$ is the number of particles with diameter $D_i$.

**Opacity Test**

The absorbances of each of the films of the different latex samples were measured with a Dual-Wavelength Flying Spot Scanning Densitometer (Shimadzu CS-9301PC) scanned under a 500 nm wavelength. Distilled water was added to the different samples to make the percent solids 18.7% uniform for all three latex samples (Table 1). Afterwards, 5.00 g of each of these diluted latex samples was mixed with 4.00 g of acrylate binder (Chemrez: R40-450 BN#030387) to form a coatings mixture. These were drawn to a uniform film using an 80 µm drawdown bar. The films were dried in the oven at 50 °C for 15 minutes. The measurements were done with the glass slides lying perpendicular to the light source and at various angles, 5.90°, 13.5°, and 17.5° relative to the horizontal plane. A clean glass slide with an acrylate binder was used as a reference and was set to a reading of zero.

**Table 1**. Target Composition of the Different Second Stage Composite Latexes.

| Stage 2 Latex *COMPOSITION* | *73/27 MMA: MAA (G)* | *66/34 MMA: MAA (G)* | *62/38 MMA: MAA (G)* |
|---|---|---|---|
| *Deionized $H_2O$* | 120.00 | 120.00 | 120.00 |
| *Seed Latex* | 3.52 | 3.52 | 3.52 |
| *APS* | 0.24 | 0.24 | 0.24 |
| *Deionized $H_2O$* | 1.42 | 1.42 | 1.42 |
| *Deionized $H_2O$* | 13.33 | 13.33 | 13.33 |
| *SDBS/other surfactants* | 0.167 | 0.167 | 0.167 |
| *MMA* | 27.80 | 27.80 | 27.80 |
| *MAA* | 8.92 | 11.90 | 14.90 |
| *EGDMA* | 0.20 | 0.20 | 0.20 |
| **Total** | **175.597** | **178.577** | **181.577** |
| Theoretical Solids (Minus $H_2O$) | 21.66% | 22.97% | 24.23% |

## RESULTS AND DISCUSSION

### Characterization of the Polymer Composites

### Infrared Spectroscopy

Figure 1 shows samples of stage 3 IR spectra where a decrease in the –O-H stretching band of PMAA in the 3500 $cm^{-1}$ region is noticeable compared with their second stage counterparts. This observation is consistent for all the spectra of stage 3 latexes, proof that there was a marked decrease in the concentration of PMAA at this stage. Furthermore, comparison of the spectra of the stage 2 latexes showed decreasing relative absorbance at 991 $cm^{-1}$ (O'Reilly et al., 1981) with increasing PMAA in the latex (Figure 2). This band assigned to the $CH_3$-O rocking vibrational frequency is a signature of the PMMA

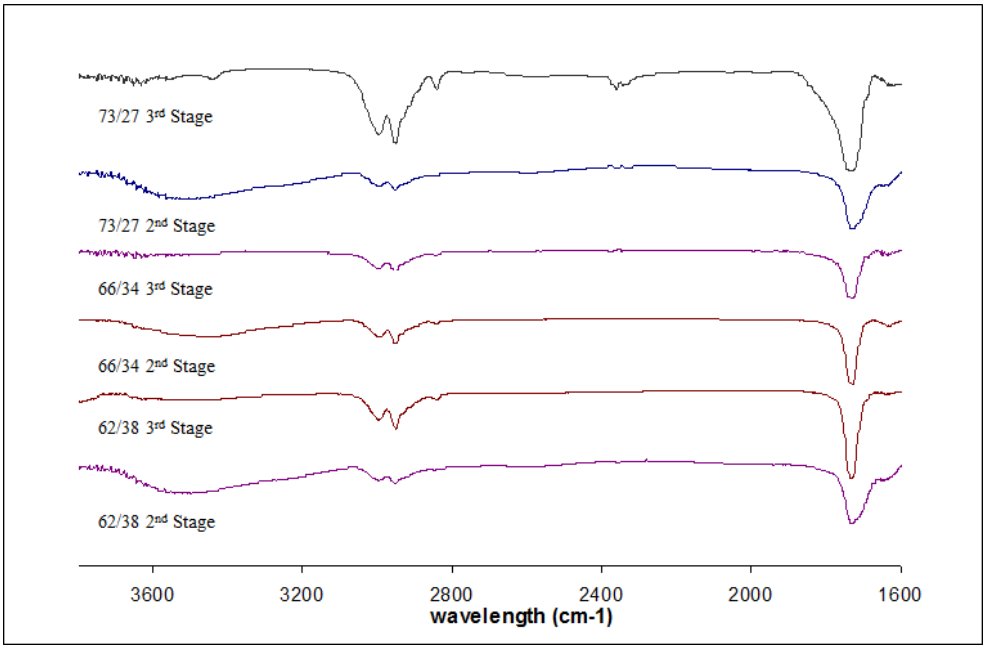


**Figure 1**. FTIR spectra of stage 2 and stage 3 latexes. The O-H stretching band at 3500 $cm^{-1}$ is observed in the spectra of all core latexes but is hardly visible in all core-shell latexes.

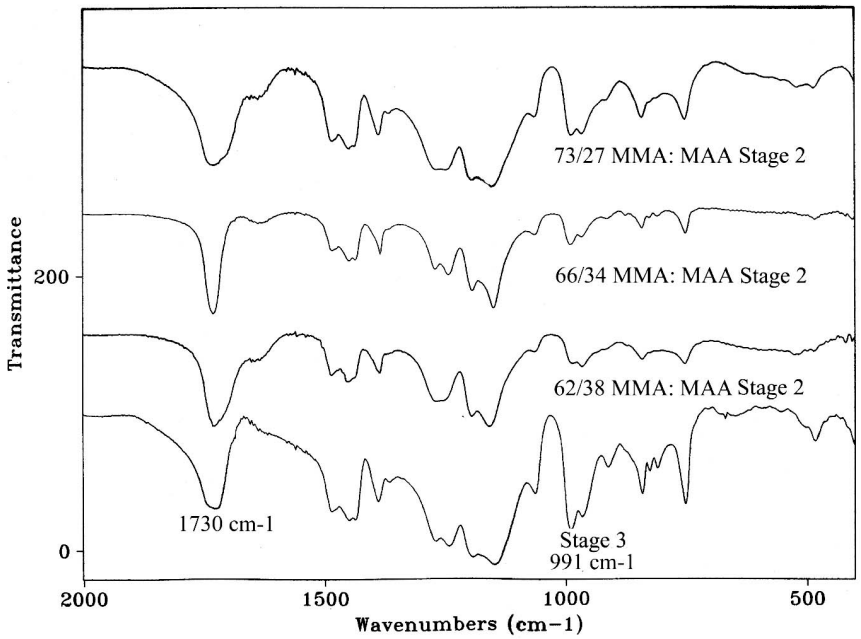


**Figure 2.** IR spectra of the different stage 2 latexes with a stage 3 latex. Each spectrum is normalized relative to the 1730 $cm^{-1}$ peak.

polymer which has methyl ester groups, and is absent in PMAA. These results confirm that the stage 2 latexes consisted mainly of P(MMA-MAA) copolymer and that it had indeed further polymerized with the PMMA in the 3rd stage latexes. The results also confirm the increasing relative PMAA concentration in the 73/27, 66/34, and 62/38 mole % MMA: MAA stage 2 latexes, respectively.

**Differential Scanning Calorimetry**

DSC studies indicate that stage 2 latex films had higher $T_g$ values than the corresponding stage 3 latexes. Table 2 shows that all the stage 2 latex films had $T_g$ values between 140-160°C. In contrast, the $T_g$ of all final stage latexes averaged 103 °C. These values are in good agreement with the calculated values of $T_g$ for copolymer blends. The higher $T_g$ of the stage 2 latex films are attributed to the presence of crosslinkers in the polymer. The $T_g$ values of the final stage latexes corroborate the FTIR results, that is, the final stage polymer particles are composed mainly of the PMMA shell since PMMA has a reported $T_g$ value of 105 °C.

Furthermore, DSC profiles also revealed increasing $T_g$ values of 141°C, 147°C, and 161°C, respectively for the 73/27, 66/34, and 62/38-mole % MMA: MAA stage 2 latex films. The higher $T_g$ observed among these polymers is indicative of higher PMAA concentration because PMAA has a high $T_g$ value of 228°C (Table 2) compared with PMMA. Therefore, the 62/38-mole% MMA:MAA stage 2 latex had the highest $T_g$ as expected from its relative high concentration of PMAA.

**Atomic Force Microscopy**

AFM images (Figure 3) using the same $Si_3N_4$ tip show that all stage 3 latex particles were almost twice as large as their corresponding stage 2 counterparts. The number average diameter measured from the AFM images for the stage 3 particles is 1.23 μm (standard deviation *s* of 0.1 μm) whereas for the stage 2 particles, diameters averaged at 0.62 μm ($s$ = 0.90 μm). These images corroborate both the FTIR and DSC results that the PMMA of the 3rd stage indeed polymerized with the stage 2 latex.

Furthermore, AFM imaging was able to show the effects of addition of surfactants on the final stage polymerization. A surfactant-free formulation during the final stage yielded a narrower distribution in size (Liu et al. 2005) of the latex particles with a uniformity index (UI) of 1.04. On the other hand, the addition of surfactants in the third stage formulation may have promoted secondary nucleation, which in turn, resulted in a wider particle size-distribution with a UI of 1.32 (Figure 4).

The AFM results imply that polymer composites were produced. The MMA, added as pure monomer during the final stage of polymerization, exhibit nonpolar character giving it greater affinity to bind and polymerize with the stage 2 particles to form its shell rather than stay in the aqueous phase. This property of MMA together with the surfactant-free environment of the third stage (final) polymerization made it conducive for polymer composite particles to form.

**$NH_4OH$ Swelling Experiments**

Addition of $NH_4OH$ to the 2nd stage and 3rd stage latexes yield different results. When $NH_4OH$ was added to stage 2 latexes, lumps of transparent, gel-like substance appeared. Analysis of these swollen 2nd stage latexes under AFM (Figure 5) revealed coagulation of particles that was not observed in their unswollen state. Further polymerization of these $NH_4OH$-treated stage 2 latex particles up to the final stage resulted in latexes that were translucent which formed clear films. The AFM image

**Table 2**. Calculated and Experimental (DSC) Glass Transition Temperatures of Polymers at Various Stages

| Polymer/Polymer Blend | 2nd Stage Latex Composition MMA: MAA mole ratio | Experimental $T_g$ (°C) | Calculated $T_g$ (°C) |
|---|---|---|---|
| 1st Stage | | 20 | -46.20[a] |
| 2nd Stage | 73/27 | 141 | 130.80[a] |
| | 66/34 | 147 | 134.71[a] |
| | 62/38 | 161 | 138.59[a] |
| 3rd Stage | 73/27 | 103 | 105.91[a] |
| | 66/34 | 103 | 105.91[a] |
| | 62/38 | 103 | 105.92[a] |
| PMMA | ___ | 105[b] | ___ |
| PMAA | ___ | 228[b] | ___ |
| PBuA | ___ | -20[b] | ___ |

[a] Calculated using the Fox equation, reference (MacDonald and Devon 2002)
[b] From reference (Park 2001)

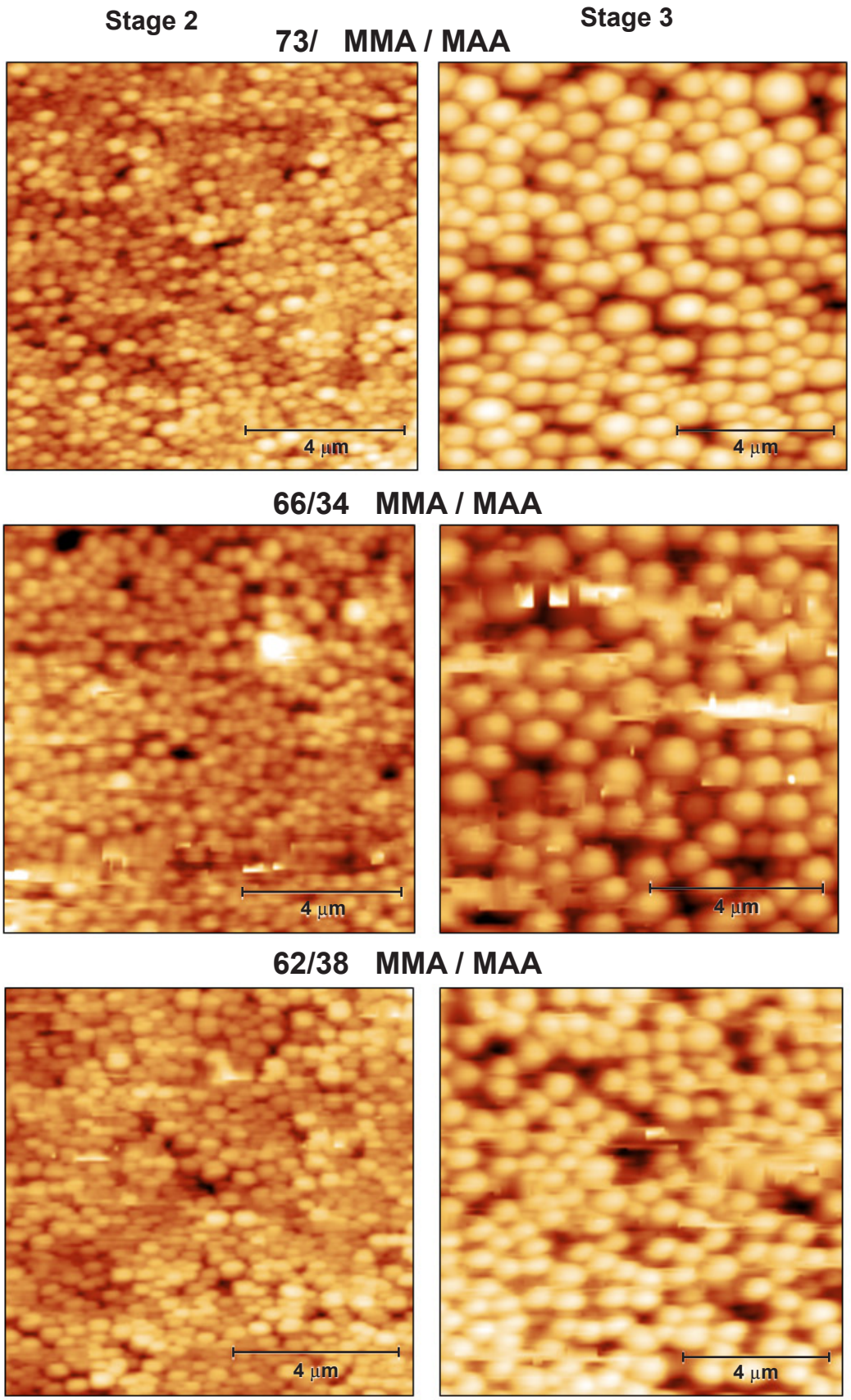


**Figure 3**. AFM images (10.0 μm x 10.0 μm) of stage 2 and stage 3 latex particles in dried films for the different formulations.

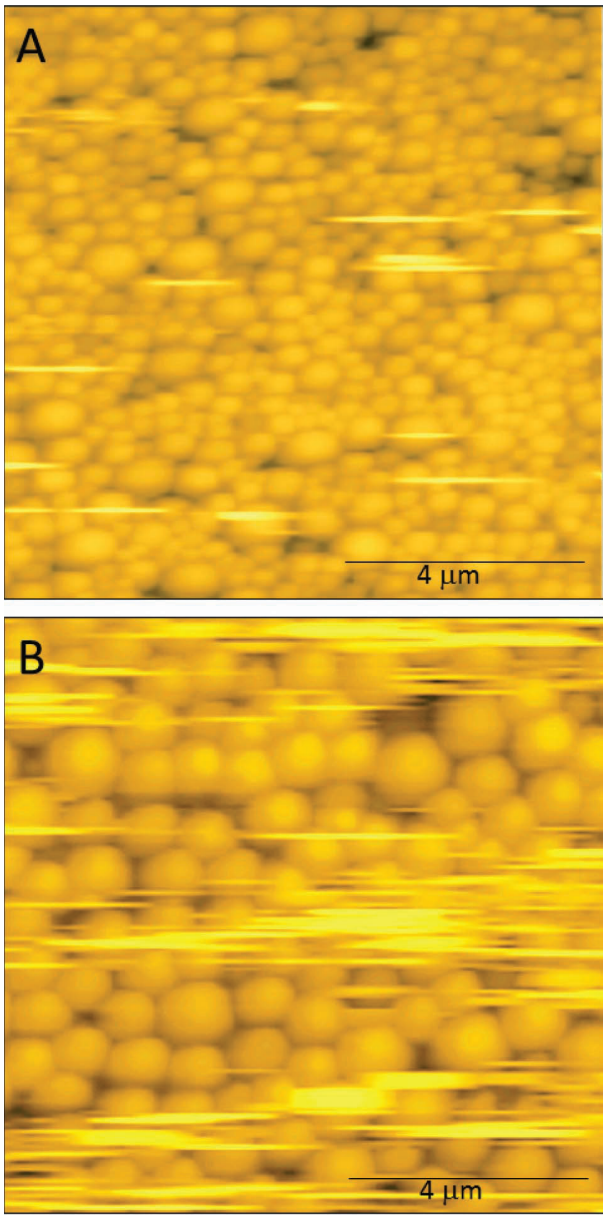


**Figure 4.** AFM images of final stage particles (10 μm x 10 μm) during stage 3 with surfactants polymerization (A) and without surfactants during stage 3 polymerization (B).

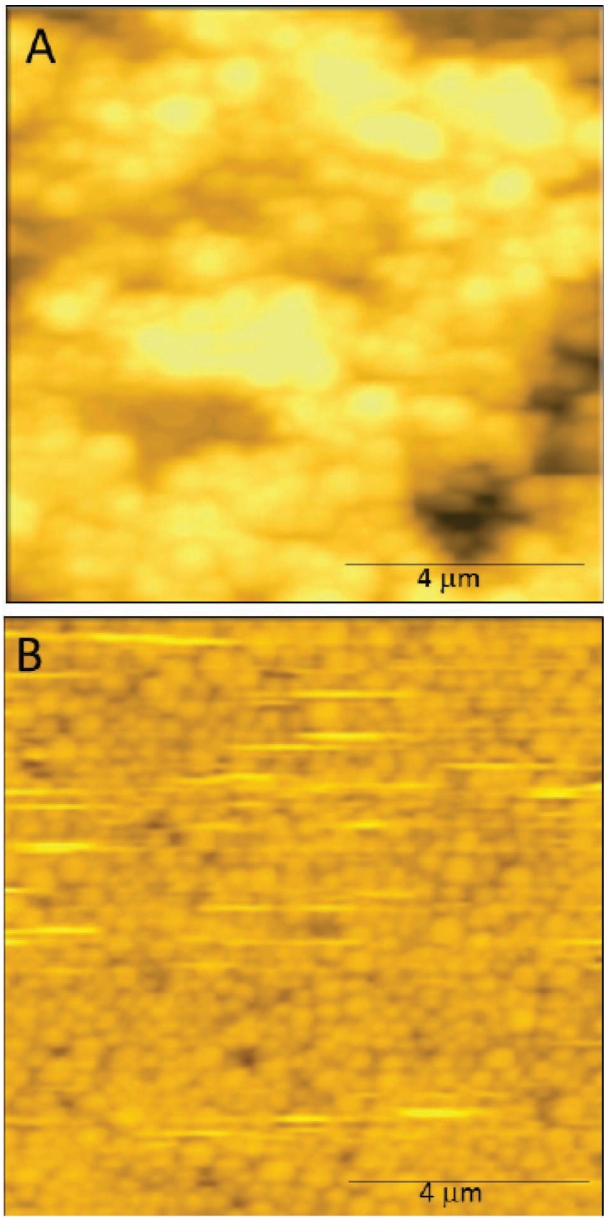


**Figure 5.** AFM images (10 μm x 10 μm) depicting stage 2 particles: coagulation of swollen particles (A) and clustering of unswollen particles (B).

(Figure 6) of these clear films revealed a flat surface and the absence of particles (at the resolution of the image), implying that the addition of the base prior to the final stage polymerization made the stage 2 particles unable to maintain their structure.

These observations can be explained by the fact that the carboxylic acid (COOH) groups in polymethacrylic acid (PMAA) of the stage 2 latex particles were neutralized by $NH_4OH$ forming carboxylate ionic groups. This, in turn, caused the ionized polymer chains to disentangle and dissolve in a polar environment such as water. The dissolution of the swollen stage 2 particles then formed a continuous film upon drying. These swollen stage 2 latex particles formed precipitates after the final stage polymerization, indicating that the MMA added at this stage polymerized separately from the stage 2 latexes, since PMMA is sparingly soluble in water.

In contrast, the addition of $NH_4OH$ to the third stage latex (*without heating*) appeared to have no effect because both the emulsion and their dried films remained opaque white.

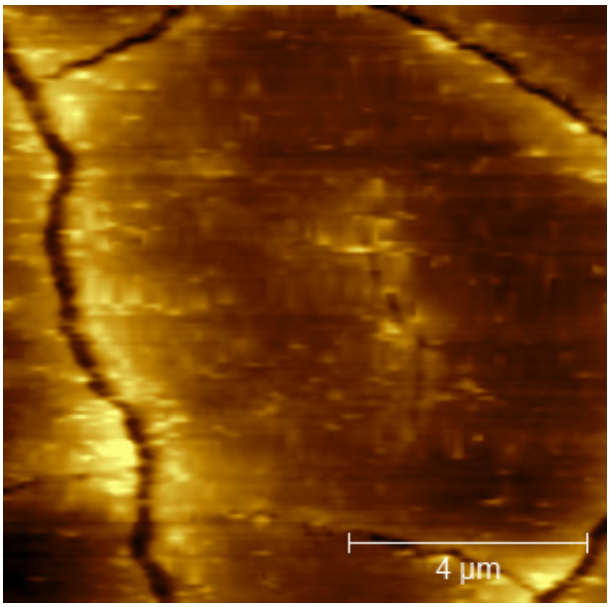


**Figure 6.** AFM image (10 µm x 10 µm) of final stage latex from $NH_4OH$-swelled stage 2 latex; note that particle formation is absent.

Furthermore, no coagulation of particles took place and the AFM images (Figure 3) revealed that the structure of these particles were intact. Moreover, should there be a substantial amount of unreacted or exposed PMAA from the stage 2 latex in the final stage polymer, the addition of a base would have still perturbed the emulsion. This hypothesis was confirmed by mixing a small amount of stage 2 latex with a stage 3 latex in a volume ratio (stage 2: stage 3) of 1: 5. This mixture indeed turned viscous when $NH_4OH$ was added and even separated into two phases when dried. Overall, these results are indicative of PMMA encapsulation of the stage 2 latex particles, following a sequential emulsion polymerization process.

## Opacity Test

The opacity of the polymer composite latex films was measured indirectly via absorbance measurements using an optical densitometer in transmission mode (Table 3). The wavelength of the tungsten light source was set to the visible spectrum region of 500 nm. As previous workers have reported (Ottewill et al. 1997) void core-shell films when dried, have interfaces between the air in the voids and the polymer resulting in the scattering of light and subsequent increase in the opacity of the material.

The sequential polymerization procedure was targeted to form a swollen MAA core-PMMA shell, which upon drying would produce a void core-shell structure. The PMMA, having a high $T_g$, should render stability to such structure. We varied the MAA content in the stage 2 polymerization to ultimately vary the void core size. Thus, the one with the highest swellable MAA content would form the largest void upon drying. For all three compositions investigated, the final polymer composition was only about 1% MAA and 99% PMMA with slight variations in the MAA content. The idea is that a large amount of swellable acrylate (PMAA) core is not needed since this ought to collapse to form the void once it dries up. The resulting void core-shell structure then provides the refractive index contrast that would enhance the opacity. It is also possible that the formed polymer consists of multiple voids encapsulated by a PMMA shell, and may not just be a core-shell structure (Okubo et al. 1992; MacDonald et al. 2002). The same multiple void structure, nonetheless, would also yield a similar enhanced opacity because of the increased number of light scattering interfaces between the voids and the polymer matrix. At this point, we could not ascertain the structure of the polymer composite in the absence of transmission electron microscope data.

The optical densitometer measures the fraction of light that is transmitted through a film: a low transmittance corresponds to high opacity. Absorption of light by the polymer and scattering by internal interfaces will decrease the optical transmission. Here, we report the total absorbance from the transmittance data, but because the sample does not absorb at the 500 nm wavelength, the transmission loss is directly attributed to scattering effects. "Absorbance" values recorded for the swollen latex particles increased with increasing PMAA concentration in the stage 2 latexes. This trend is consistent even when the film mixtures were positioned and scanned at different angles relative to the horizontal plane: 5.90°, 13.5°C, and 17.5° (Figure 7). This difference in "absorbance" may be attributed to the different MMA: MAA stage 2 latex formulations. The difference in MMA: MAA stage 2 concentrations in polymer composite la-

**Table 3**. Summary of Densitometry Absorbance Readings at Various Angles of Incidence, Tungsten Lamp, λ= 500 nm

| *ABSORBANCE (STANDARD DEVIATION) IN A.U.* | | | |
|---|---|---|---|
| **Scan Angles (degrees)** | **MMA:MAA Composition (Mole Ratio)** | | |
| | **73/27** | **66/34** | **62/38** |
| 0 | 0.010 (0.002) | 0.021 (0.002) | 0.034 (0.002) |
| 5.90 | 0.019 (0.002) | 0.031 (0.002) | 0.039 (0.002) |
| 13.5 | 0.032 (0.002) | 0.040 (0.002) | 0.0047 (0.002) |
| 15.7 | 0.056 (0.003) | 0.061 (0.002) | 0.074 (0.002) |

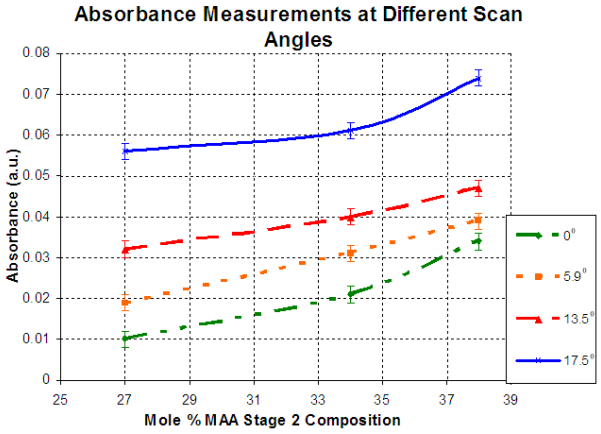


**Figure 7.** Densitometer absorbance measurements at λ = 500 nm of swollen final stage (stage 3) latexes with varying stage 2 composition.

texes altered the scattering power of the film mixture. The 62/38 MMA: MAA 2nd stage composition in the final polymer composite latex produced the highest light scattering. Since other factors affecting light scattering such as percent solids and particle size were kept constant, the opacity of such enhancers may be attributed to either the larger void core-shell interfaces, if core-shell structures were indeed formed, or in the case of multiple interfacial sites, greater number of void interfaces. Both scenarios translate to greater light scattering.

In summary, the composite latex with a 62/38 MMA: MAA 2nd stage composition, which had the highest concentration of PMAA in the stage 2 latex, produced the highest scattering power and consequently, the highest opacity among the three latexes.

## CONCLUSIONS

A three-stage sequential polymerization made up of MMA, MAA, and BuA monomers was formulated and made into polymer composite latexes with different MMA: MAA stage 2 compositions. The success of the sequential polymerization was confirmed by a combination of FTIR, $T_g$ measurements, AFM imaging, and $NH_4OH$ swelling studies.

Optical densitometry experiments showed that the scattering (measured in "absorbance" units) of the P(MMA-MAA-BuA)-PMMA polymer composite latex increased with increasing PMAA/PMMA polymer ratio in the 2nd stage when force-swelled with $NH_4OH$. This increase in scattering is indicative of an increase in the opacity of the latex films and thereby establishes a correlation between opacity and PMAA concentration in the 2nd stage for these systems.

## ACKNOWLEDGMENTS

The authors would like to thank the CHED-COE for partial support of this project and Chemrez, Inc. for their generosity in donating the necessary chemicals for this work.

## REFERENCES

CAO TY, XU YS, CAO JW, MIAO AH, YUAN CD. 2005. Preparation of monodispersed hollow polymer particels by seeded emulsion polymerization under low emulsifier conditions. J Appl Polymer Sci 98: 1505-1510.

DIMONIE VL, DANIELS ES. 1997. In: Emulsion Polymerization and Emulsion Polymers. Lovell PA, El- Asser MS. (ed.). Chichester, England: John Wiley and Sons. p. 294-326.

DOLUI SK, RAY BC, KHAN AK. 2008. Preparation of core-shell emulsion polymer and optimization of shell composition with respect to opacity of paint film. Progress in Organic Coatings 62: 65-70.

EL-ASSER M, SUDOL ED. 1997. In: Emulsion Polymerization and Emulsion Polymers. Lovell PA, El- Asser MS. (ed.). Chichester, England: John Wiley and Sons. p. 37-55

KASPER A, BARTSCH E, SILLESCU E. 1998. Self-diffusion in concentrated colloid suspensions studied by digital video microscopy of core−shell tracer particles. Langmuir 14: 5004-5010

KIRSCH S, DOERK A, BARTSCH E, SILLESCU H. 1999. Synthesis and characterization of highly cross-linked, monodisperse core−shell and inverted core−shell colloidal particles. Polystyrene/poly(tert-butyl acrylate) core−shell and inverse core−shell particles. Macromolecules 32: 4508-4518

KLUMPERMAN B, DE WET-ROOS D, SANDERSON RD, VAN ZYL AJP. 2003. Macromolecules. 36: 8621-8629.

KOWALSKI A, VOGEL M. 1984. Sequential heteropolymer dispersion and a particulate material obtainable therefrom, useful in coating compositions as an opacifying agent. Rohm and Haas Company: United States. US Patent Reference # 4469825.

LANDFESTER K, BOEFFEL C, LAMBLA M, SPIESS HW. 1996. Characterization of interfaces in core−shell polymers by advanced solid-state NMR methods. Macromolecules 29: 5972-5980.

LIU DS, LI YZ, DU Y, KAN CY, KANG K. 2005. A new kind of void soap-free P(MMA- EA-MAA) latex particles. Chin Chem Lett 16: 831-834

MACDONALD C, DEVON M. 2002. Hollow latex particles: synthesis and applications. Advances in Colloid and Interface Science 99: 181-213.

OH KJ, KIM D-S, LEE JH, CHOI K-Y, LEE C. 2003. Preparation of Nanocapsules Containing Phase Change Materials by Miniemulsion Polymerization. Journal of the Korean Chemical Society. pp.39-42.

OKUBO M, ICHIKAWA K, FUJIMARA M. 1992. In ACS Symposium Series Polymer Latexes Preparation, Characterization, and Applications; Daniels E. (ed.). Washington DC: American Chemical Society: p. 282-288.

O'REILLY JM, MOSHER RA. 1981. Conformational energies of stereoregular poly(methyl methacrylate) by Fourier transform infrared spectroscopy. Macromolecules 14: 602-608.

OTTEWILL RH, SCHOFIELD AB, WATERS AJ, WILLIAMS NStJ. 1997. Preparation of Core-shell Colloid Particles by Encapsulation. Colloid and Polymer Science 275: 274-283.

PARK JM. 2001. Core-shell polymerization with hydrophilic polymer cores. Korean Polymer J. 1: 51-65.

SUNBERG DC, STUBBS JM. 2008. Core-shell and other multiphase latex particles—confirming their morphologies and relating those to synthesis variables. J Coat Technol Res 5: 169-180.

VANDERHOFF JW, PARK J, EL-ASSER M. In: ACS Symposium Series Polymer Latexes Preparation, Characterization, and Applications. Daniels E. (ed.) Washington DC: American Chemical Society. p. 272-281.

VANDERHOFF JW, PARK JM, EL ASSER MS. 1992. In: Polymer Latexes: Preparation, Characterization, and Applications. Daniels ES, Sudol ED, El Asser MS. (eds.). Preparation of Particles for Microvoid Coatings by Seeded Emulsion Polymerization. ACS Symposium Series No. 492, Chapter 17 pp. 272-281.

WINNIK MA. 1997. In: Emulsion Polymerization and Emulsion Polymers; Lovell PA, El-asser Mohammed S (ed.). Chichester, England: Wiley and Sons. p. 467-515.

ZHONG ZY, OU YC, QI ZN, HU GH. 1998. Toughening of nylon 6 with a maleated core-shell impact modifier. J Polymer Science B: Polymer Physics 36: 1987-1994.